Petroleum Science 23 (2026) 5561–5571

Contents lists available at ScienceDirect

Petroleum Science

journal homepage: www.keaipublishing.com/en/journals/petroleum-science

Original Paper

A prediction method for safe mud density of natural gas hydrate reservoirs under temperature-pressure dual control

Lin Dong [a], Neng-You Wu [a,b], Ke Ke [c], Li-Lin Li [c], Yong-Chao Zhang [b], Yan-Long Li [a,*]

[a] Laoshan Laboratory, Qingdao, 266237, Shandong, China
[b] Key Laboratory of Gas Hydrate, Ministry of Natural Resources, Qingdao Institute of Marine Geology, Qingdao, 266237, Shandong, China
[c] Sinopec Research Institute of Petroleum Engineering, Beijing, 100101, China

ARTICLE INFO

Article history:
Received 15 September 2025
Received in revised form
31 March 2026
Accepted 8 April 2026
Available online 13 April 2026

Edited by Jia-Jia Fei

Keywords:
Natural gas hydrate
Safe mud density window
Temperature sensitivity
Wellbore stability
Hydrate dissociation

ABSTRACT

Wellbore instability is one of the most encountered issues during hydrate exploration, which correlates with mud density and temperature. However, current studies ignore the effect of mud temperature on safe mud density windows, leading it fails to meet requirements of sufficient drilling in hydrate reservoirs. Herein, we propose a new model to predict safe mud density windows by introducing temperature-pressure dual control, which is more accurate and applicable for hydrate reservoirs. Collapse pressure equivalent density decreases 6.19% while fracture pressure equivalent density increases 4.52% with hydrate saturation rising from 0 to 50% under normal conditions. Hydrate formation can narrow the safe mud density window significantly. Equivalent density of collapse pressure presents temperature sensitivity, especially mud temperature ranging from 287.9 to 289.3 K. Hydrate dissociation can narrow the safe mud density window by ~27% on average with hydrate saturation of 50%, which will be magnified with increasing intermediate principal stress. On this basis, an integrated control system involving temperature-pressure dual control is established to deal with potential drilling risks of multi-layer hydrate reservoirs. This work provides new insights into safe mud density windows dependent on temperature and presents design principles for sufficient drilling in natural gas hydrate reservoirs.

1. Introduction

Wellbore instability is a fundamental problem encountered in natural gas hydrate exploration and exploitation, which may further reduce drilling efficiency and increase engineering geological risks (Dong et al., 2022b; Gizatullin et al., 2023). Various well types have been applied in hydrate drilling with increasing demand for hydrate productivity in trial production (Lu et al., 2023; Wani et al., 2023; Dong et al., 2024c). That brings in a higher requirement in risk evaluation and wellbore stability control (Al-Shami et al., 2023; Dong et al., 2024c; Tian et al., 2024). Distinct from conventional oil and gas reservoirs, hydrate formation is shallow, low-strength, and unconsolidated, resulting in insufficient understanding of wellbore failure mechanisms (Yoneda et al., 2019; Dong et al., 2024d). In this regard, it is urgent to investigate wellbore issues and further propose stability control strategies.

Wellbore stability primarily correlates to drilling mud property, stress states around the borehole, as well as formation strength (Dong et al., 2024b; Wei et al., 2025). The hole collapse/shrinkage will occur with a smaller mud weight, while the leakage/fracture may appear with a higher one (Zhang, 2013; Bagdeli et al., 2019), as displayed in Fig. 1. In this regard, proper mud density can maintain wellbore stability with accurate control of bottom hole pressure and mud circulation during drilling hydrate. In particular, invaded drilling mud with higher temperature can lead to massive hydrate dissociation and further reservoir strength reduction, causing changes in designed safe mud density windows (Zheng et al., 2020; Wan et al., 2023). Conversely, hydrate dissociation induces a temperature drop of circulating drilling mud in boreholes, resulting in potential drilling risks (Huang et al., 2020a; Abdelhafiz et al., 2023). Generally, hydrate layers exhibit temperature sensitivity during the drilling process (Gong et al., 2025; Zhang et al., 2025). However, a better understanding of the temperature-dependent safe mud density window and wellbore stability in hydrate reservoirs remains an unclear and open topic.

* Corresponding author.
E-mail address: ylli@qnlm.ac (Y.-L. Li).
Peer review under the responsibility of China University of Petroleum (Beijing).

https://doi.org/10.1016/j.petsci.2026.04.012
1995-8226/

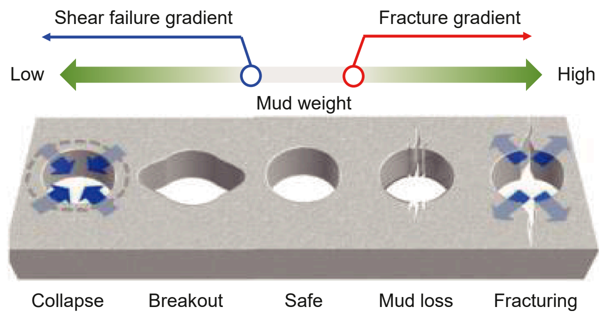

Fig. 1. Relation between the drilling mud window and wellbore states, modified from (Zhang, 2013; Bagdeli et al., 2019).

Safe mud density windows have been involved in safe and efficient drilling in hydrate reservoirs, especially collapse/fracture pressure prediction and mud density window design. Generally, drilling mud invasion and corresponding hydrate dissociation can alter wellbore status, favoring the rule that temperature can affect the drilling mud density range (Sun et al., 2018; Huang et al., 2020b; Dong et al., 2023b). In addition, Li et al. develop an analytical model and state that higher mud flow rate results in lower collapse/fracture pressure (Li et al., 2020). Besides, the lower borehole enlargement rate corresponds to higher mud density, indicating that mud weight design must consider the borehole enlargement (Li et al., 2024; Fan et al., 2025). After that, the lower limit of the mud density window for hydrate reservoirs is temperature sensitive and relates to formation strength, leaving unclear of the upper limit versus temperature (Li and Wu, 2022). Moreover, collapse pressure equivalent density could become higher, and instability risks would be amplified with hydrate dissociation (Dong et al., 2023b; Sun et al., 2022). However, these studies focus on mud weight range, ignoring the effect of mud temperature on the safe mud density window during drilling hydrate reservoirs.

Herein, we establish a new model for safe mud density of gas hydrate reservoirs under temperature-pressure dual control, considering the effect of hydrate dissociation on wellbore states. The temperature sensitivity of both collapse and fracture pressure equivalent density is investigated to challenge determining the lower and upper limit of the safe mud density window in view of hydrate-dissociation induced drilling risks. After that, an integrated mud system involved in temperature-pressure dual control is established to deal with drilling issues in multi-layer hydrate reservoirs. This work can provide a reference for drilling mud density window design and wellbore stability control in natural gas hydrate reservoirs.

2. Model

2.1. Calculation method

Natural gas hydrate reservoirs are totally different from traditional oil and gas formations due to the varying strength and stiffness after the hydrate phase transition. These dissociation-induced transitions will lead to changes in the lower and upper limit of safe mud density windows that represent equivalent density of collapse and fracture pressure. Thus, we develop a new model for safe mud density windows under temperature-pressure dual control to deal with the temperature-sensitive issues, as depicted in Fig. 2. Wherein, collapse and fracture pressure equivalent density dependent on mud temperature are obtained with the new proposed model, which provides a basis for establishing safe mud density windows applied in hydrate reservoirs.

Compared with current models proposed for oil and gas reservoirs, this model exhibits two fundamental advantages. One is correlating the mud density with hydrate saturation that supports the accurate prediction of collapse and fracture pressure, resulting in a broader application scope. The other is introducing the effect of temperature into the prediction model, which improves the prediction precision of the safe mud density window for hydrate reservoirs.

Additionally, basic assumptions have been involved to simplify the calculation and improve efficiency: (1) The reservoir only contains methane hydrate with homogeneous distribution. (2) The drilling fluid invasion is a transient process without mud cake formation. (3) Hydrate will dissociate once the temperature exceeds the phase equilibrium.

2.2. Stress around boreholes

Stress states around the drilled borehole are the basis and precondition of wellbore state evaluation and drilling mud density window design. To obtain principal stresses, transformation relations among the in-situ coordinate system, geographic coordinate system, as well as borehole coordinate system (see Fig. 3.) are required, which promotes solving the engineering problems through numerical calculations.

Stress states of the in-situ coordinate system differ from that of the geographic coordinate system, which needs to be transformed mathematically by introducing Euler angles (α, β, γ), as displayed in Fig. 3(a). The transformation process can be characterized by Eqs. (1–3).

$$[\boldsymbol{\sigma}_{\mathrm{s}}] = \begin{bmatrix} \sigma_x & 0 & 0 \\ 0 & \sigma_y & 0 \\ 0 & 0 & \sigma_z \end{bmatrix} \tag{1}$$

$$[\boldsymbol{\sigma}_{\mathrm{s}}] = [\boldsymbol{R}_{\mathrm{s}}][\boldsymbol{\sigma}_{\mathrm{e}}]\left[\boldsymbol{R}_{\mathrm{s}}^{\mathrm{T}}\right] \tag{2}$$

$$[\boldsymbol{R}_{\mathrm{S}}] = \begin{bmatrix} \cos\alpha\cos\beta & \sin\alpha\cos\beta & -\sin\beta \\ \cos\alpha\sin\beta\sin\gamma - \sin\alpha\cos\gamma & \sin\alpha\sin\beta\sin\gamma - \cos\alpha\cos\gamma & \cos\beta\sin\gamma \\ \cos\alpha\sin\beta\cos\gamma - \sin\alpha\sin\gamma & \sin\alpha\sin\beta\cos\gamma - \cos\alpha\sin\gamma & \cos\beta\cos\gamma \end{bmatrix} \tag{3}$$

where σ_x, σ_y, and σ_z represent the in-situ stresses, MPa, $[\boldsymbol{R}_{\mathrm{s}}]$ is the transformation matrix, dimensionless, and $[\boldsymbol{\sigma}_{\mathrm{e}}]$ denotes the stress tensor in the geographic coordinate system, MPa.

Similarly, stresses should be transformed from the geographic coordinate system to the borehole coordinate system without assuming the borehole normal to the near-wellbore formation. Key factors in this transformation are the inclination angle δ and azimuth Ψ, which can be applied to identify the stress tensor $[\boldsymbol{R}_2]$. These relations are written in Eqs. (4) and (5). After that, the stress solutions can be obtained to analyze the wellbore stability (Aadnoy and Chenevert, 1987).

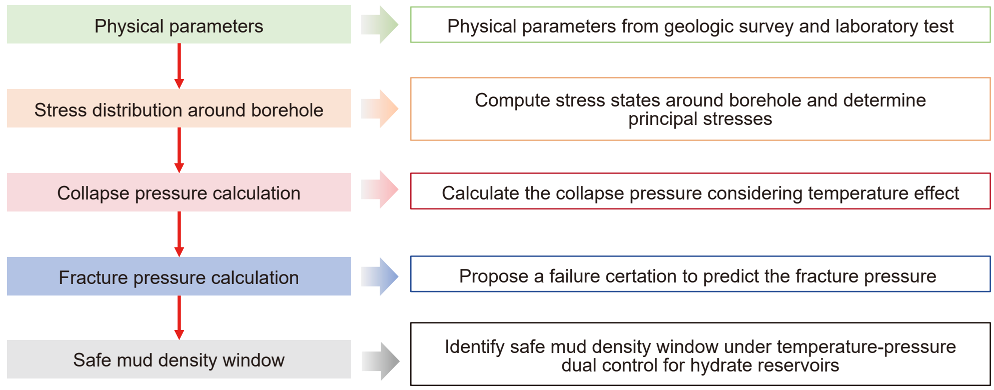

Fig. 2. Flowchart for calculating the safe mud density windows of hydrate reservoirs under temperature-pressure dual control.

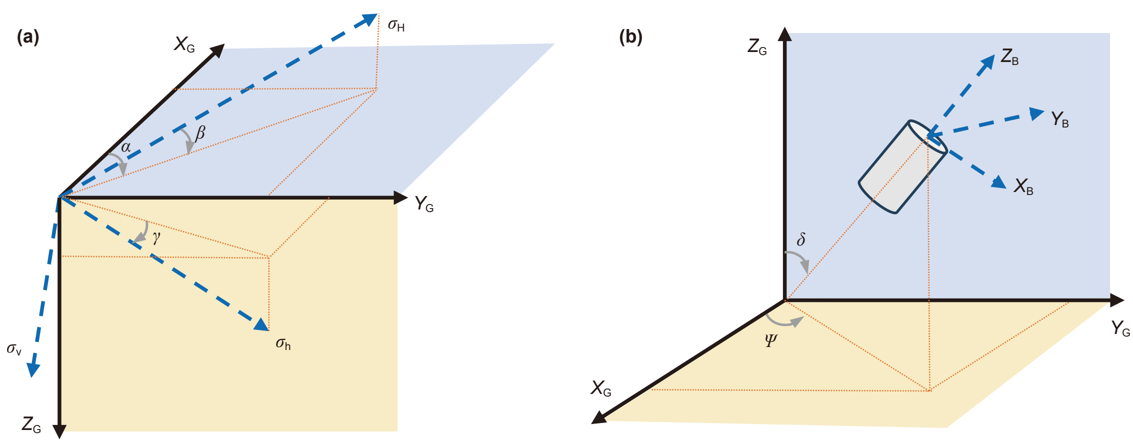

Fig. 3. Illustration of the coordinate transformation revised from (Li, 2022). (**a**) Transformation between the in-situ stress coordinate and geographic coordinate, and (**b**) transformation between the geographic coordinate and the borehole coordinate. X_G, Y_G, and Z_G present X-axis, Y-axis, and Z-axis of the geographic coordinate system, while X_B, Y_B, and Z_B are that of the borehole coordinate system.

$$[\boldsymbol{\sigma}_\mathrm{b}] = [\boldsymbol{R}_2][\boldsymbol{\sigma}_\mathrm{e}]\left[\boldsymbol{R}_2^\mathrm{T}\right] = \begin{bmatrix} \sigma_{xx} & \sigma_{xy} & \sigma_{xz} \\ \sigma_{yx} & \sigma_{yy} & \sigma_{yz} \\ \sigma_{zx} & \sigma_{zy} & \sigma_{zz} \end{bmatrix} \tag{4}$$

$$[\boldsymbol{R}_2] = \begin{bmatrix} \cos\delta\cos\psi & \sin\delta\cos\psi & -\sin\psi \\ -\sin\delta & \cos\delta & 0 \\ \cos\delta\sin\psi & \sin\delta\sin\psi & \cos\psi \end{bmatrix} \tag{5}$$

where δ and Ψ represent the inclination angle and azimuth, rad, and $[\sigma_\mathrm{b}]$ is the stress tensor in the geographic coordinate system, MPa.

Based on the wellbore stability mechanics theory, it is convenient to identify the stress states in the borehole coordinate system. In this regard, stressful solutions can be expressed as:

$$\begin{aligned} &\sigma_r = P_\mathrm{m} - P_\mathrm{p} \\ &\sigma_\theta = \sigma_{xx} + \sigma_{yy} - 2(\sigma_{xx} - \sigma_{yy})\cos 2\theta - 4\sigma_{xy}\sin 2\theta - P_\mathrm{m} - P_\mathrm{p} \\ &\sigma_z = \sigma_{zz} - 2v\left[(\sigma_{xx} - \sigma_{yy})\cos 2\theta + 2\sigma_{xy}\sin 2\theta\right] - P_\mathrm{p} \\ &\tau_{\theta z} = 2(\sigma_{yz}\cos\theta - \sigma_{xz}\sin\theta) \end{aligned} \tag{6}$$

where σ_r, σ_θ, σ_z, and $\tau_{\theta z}$ are the radial, hoop, vertical, and tangential stress at a specific point of wellbore, MPa, v is the Poisson's ratio, dimensionless, θ represents the polar angle, °, P_p denotes the pore original pressure of the hydrate reservoir, MPa, and P_m represents the borehole pressure, MPa.

On the basis, principal stresses of near wellbore formation can be obtained by Eq. (7).

$$\begin{cases} \sigma_i = \sigma_r \\ \sigma_j = \dfrac{1}{2}(\sigma_\theta + \sigma_z) + \dfrac{1}{2}\left[(\sigma_\theta - \sigma_z)^2 + 4\tau_{\theta z}^2\right]^{1/2} \\ \sigma_k = \dfrac{1}{2}(\sigma_\theta + \sigma_z) - \dfrac{1}{2}\left[(\sigma_\theta - \sigma_z)^2 + 4\tau_{\theta z}^2\right]^{1/2} \end{cases} \tag{7}$$

where σ_i, σ_j, and σ_k are the principal stress tensor of near-wellbore formation, MPa.

After that, Eq. (8) states the calculation of the maximum and minimum principal stresses.

$$\begin{aligned} \sigma_1 &= \max\left(\sigma_i, \sigma_j, \sigma_k\right) \\ \sigma_3 &= \min\left(\sigma_i, \sigma_j, \sigma_k\right) \end{aligned} \tag{8}$$

where σ_1 and σ_3 are the maximum and minimum principal stresses, MPa.

2.3. Collapse pressure

The Druck-Prager criterion is a kind of discriminant rule that is widely applied in determining wellbore stability in drilling natural gas hydrate reservoirs (Dong et al., 2020; Zhao et al., 2025). Based on Druck-Prager criterion, we developed a collapse pressure model by introducing hydrate saturation and intermediate principal stress, as given in Eqs. (9–11). On this basis, the lower limit of the safe mud density window is obtained to favor the drilling process in hydrate reservoirs.

$$f(P_m) = K_f(S_h) + \beta(S_h)I_1 - \sqrt{J_2} \tag{9}$$

$$J_2 = \frac{1}{6}\left[(\sigma_1-\sigma_2)^2 + (\sigma_1-\sigma_3)^2 + (\sigma_2-\sigma_3)^2\right] \tag{10}$$

$$I_1 = \sigma_1 + \sigma_2 + \sigma_3 \tag{11}$$

where I_1 and J_2 represent the first invariant function of the effective stress tensor and second invariants of the stress deviator, MPa, K_f and β are the model coefficients, which relate to hydrate saturation S_h, dimensionless.

According to previous studies (Zhang et al., 2015; Dong et al., 2020), Eq. (9) can be transformed by assuming that $f(P_m)$ is a function of hydrate saturation and effective confining pressure.

$$f(P_m) = A(S_h) + B(S_h)\sigma_3 - \sigma_1 \tag{12}$$

$$A(S_h) = 0.0313S_h + 2.58 \tag{13}$$

$$B(S_h) = 1.701\ \exp(0.0182S_h) \tag{14}$$

where $A(S_h)$ and $B(S_h)$ can be identified by referring to previous studies (Dong et al., 2020, 2022a).

Specifically, the collapse pressure P_{col} can be calculated through the Newton-Simpson method. The collapse pressure equals the obtained drilling mud pressure when the yield area is not larger than the 3.0% borehole area (Li, 2022; Li et al., 2024).

2.4. Fracture pressure

Equivalent density of fracture pressure services as the lower limit of the safe mud density window for drilling hydrate reservoirs. With consideration of the reservoir characteristic and strength theory, a calculation method of fracture pressure is proposed for hydrate reservoirs, wherein the fracture pressure correlates to hydrate saturation as well as stress states (Too et al., 2018; Zhong et al., 2024). This model is simple, effective, and applicable, which is given by Eqs. (15–18).

$$P_f = 3\sigma_h - \sigma_H - \alpha P_p + S_t \tag{15}$$

$$S_t = C(S_h)/\tan\phi(S_h) \tag{16}$$

$$C = C_0\ \exp(0.0208S_h) \tag{17}$$

$$\phi = \phi_0 + 0.189S_h \tag{18}$$

where P_f and P_p represent the fracture pressure and pore pressure of reservoirs, respectively, MPa, S_t is the tensile strength determined through empirical formulas, MPa, σ_H and σ_h are the maximum and minimum principal stresses, respectively, MPa, C and C_0 denote the cohesion of sediments with and without hydrate, MPa, ϕ and ϕ_0 are called the internal friction angle of hydrate-bearing and hydrate-free sediments, respectively, °, and α is called the effective stress coefficient, dimensionless.

3. Drilling mud density window

3.1. Effect of mud temperature

Proper pressure and temperature conditions are needed to permit hydrate existing stably in the near-wellbore reservoir, as depicted by Fig. 4. The stability margin can be characterized by the phase equilibrium curve of gas hydrate, in which the relation between pressure and temperature is given by:

$$P_{eq} = 9 \times 10^{-14} e^{0.1136T_{eq}} \tag{19}$$

where P_{eq} represents the equilibrium pressure, MPa, and T_{eq} is the equilibrium temperature, K.

To keep the gas hydrate from dissociation, the lower limit of drilling mud density is identified based on the collapse pressure and equilibrium pressure. This lower limit of drilling mud density ρ_{low} can be expressed as:

$$\begin{cases} \rho_{low} = \dfrac{\max(P_{col}, P_{eq})}{gH} & P_{eq} < P_f \\ \rho_{low} = \dfrac{P_{col}(S_h = 0)}{gH} & P_{eq} \geq P_f \end{cases} \tag{20}$$

where P_{col} is the collapse pressure, MPa, g represents the gravitational acceleration, m/s^2, and H is called the vertical depth, m.

Similarly, the upper limit also depends on the equilibrium pressure, reflecting the effect of hydrate dissociation. This upper limit of drilling mud density is the fracture pressure with hydrate saturation equal to 0 once the hydrate dissociates. Thus, the upper limit of drilling mud density ρ_{up} can be given by:

$$\begin{cases} \rho_{up} = \dfrac{P_f}{gH} & P_{eq} < P_f \\ \rho_{up} = \dfrac{P_f(S_h = 0)}{gH} & P_{eq} \geq P_f \end{cases} \tag{21}$$

3.2. Model domain and boundary conditions

Fig. 5 exhibits the geometry of the borehole trajectory in the hydrate reservoir. It refers to the site SH2 located in the Shenhu area of the South China Sea (Wan et al., 2018; Dong et al., 2023a). The hydrate layer with a thickness of 44 m exists about 185 m below the sea floor, which only contains hydrate and water. The hydrate saturation is 35% and the porosity is 0.40. A vertical well is located in the center of the target reservoir with a diameter of 0.44 m.

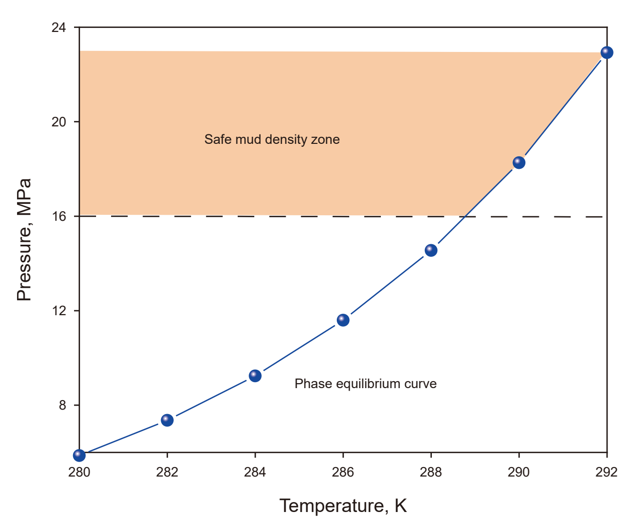

Fig. 4. Phase equilibrium curve of hydrate and safe pressure range.

The target reservoir properties and boundary conditions are obtained from geological survey data and test outcomes of drilled cores (Wan et al., 2018; Dong et al., 2023a), as listed in Table 1.

3.3. Calculation process of safe mud density window

The mud density window obtained from this proposed approach mainly depends on mud temperature and pressure, rather than a single mud pressure. Both upper and lower limits change complicatedly due to the varying equilibrium pressure of hydrate versus temperature.

Herein, we show three steps to identify the upper and lower limits under the temperature-pressure dual control. First, obtain the stress states of hydrate reservoirs around the drilled borehole based on geological data, physical parameters, as well as stress model. Then, calculate the collapse and fracture pressure by considering the effect of temperature on hydrate dissociation. Finally, identify the safe drilling mud density window under the temperature-pressure dual control. The detailed calculation process of the safe drilling mud density window is provided in Fig. 6.

4. Results and discussion

4.1. Safe mud density window without considering temperature

In general, the safe mud density window primarily depends on hydrate saturation as well as stress states without reaching phase equilibrium conditions. Fig. 7 displays the safe mud density window of hydrate reservoirs with original hydrate saturation from 0 to 50%. There is a downtrend of collapse pressure equivalent density ranging from 1.06 to 0.99 g/cm^3, while an opposite tendency of fracture pressure equivalent density with a scope of 1.31–1.38 g/cm^3. These outcomes lie in a reasonable scope compared to previous studies (Motghare and Musale, 2017; Cheng et al., 2019; Li et al., 2020; Sun et al., 2022; Li and Wu, 2022), verifying the accuracy and applicability of this proposed model, as shown in Fig. 7(c) and (d). Besides, collapse pressure equivalent density decreases 6.19% while fracture pressure equivalent density increases 4.52% with original hydrate saturation rising from 0 to 50%.

Be noted that, calculated lower and upper limits alter with the model coefficients and physical parameters. That is the fundamental cause of obvious differences in various calculated results

Table 1
Parameters used in this proposed model.

Parameter	Value
Borehole radius, a	0.22 m
Pore pressure, P_p	14.3 MPa
Vertical stress, σ_v	16.3 MPa
Maximum horizontal stress, σ_H	15.8 MPa
Minimum horizontal stress, σ_h	15.3 MPa
Formation temperature, T	287.94 K
Hydrate saturation, S_h	35%
Water saturation, S_w	65%
Cohesion (hydrate-free), C_0	0.4378 MPa
Internal friction angle (hydrate-free), ϕ_0	0.189 rad
Effective stress coefficient, α	0.9
Porosity	0.4

(Moos et al., 2003; Gholami et al., 2015). In this respect, this model must be improved and optimized continuously for higher precision based on field data as well as laboratory experiments.

4.2. Effect of temperature on safe mud density window

Mud temperature can alter the safe mud density window of hydrate reservoirs in two aspects: one is affecting the lower limit, collapse pressure equivalent density, and the other is changing the whole mud density window. These phenomena are mainly determined by differences between the mud temperature and hydrate equilibrium temperature.

Only the lower limit of safe mud density window varies when the equilibrium temperature is higher than the collapse pressure and less than the fracture pressure. To be specific, collapse pressure equivalent density rises while the fracture pressure equivalent density remains constant. It results in a narrower window with a larger value of the lower limit, as exhibited in Fig. 8. For example, collapse pressure equivalent density is changed to 1.02 g/cm^3 with hydrate saturation no less than 23.9%, instead of the original values.

In addition, collapse pressure increases from 14.4 to 17 MPa with mud temperature rising from 287.9 to 289.3 K, indicating obvious temperature sensitivity. There is a need to increase pressure for preventing phase transition because higher temperature of invaded drilling mud can cause hydrate dissociation. Up to a point, the higher mud temperature permits larger dissociation rate of hydrate in pores. Notably, however, the mud invasion process is

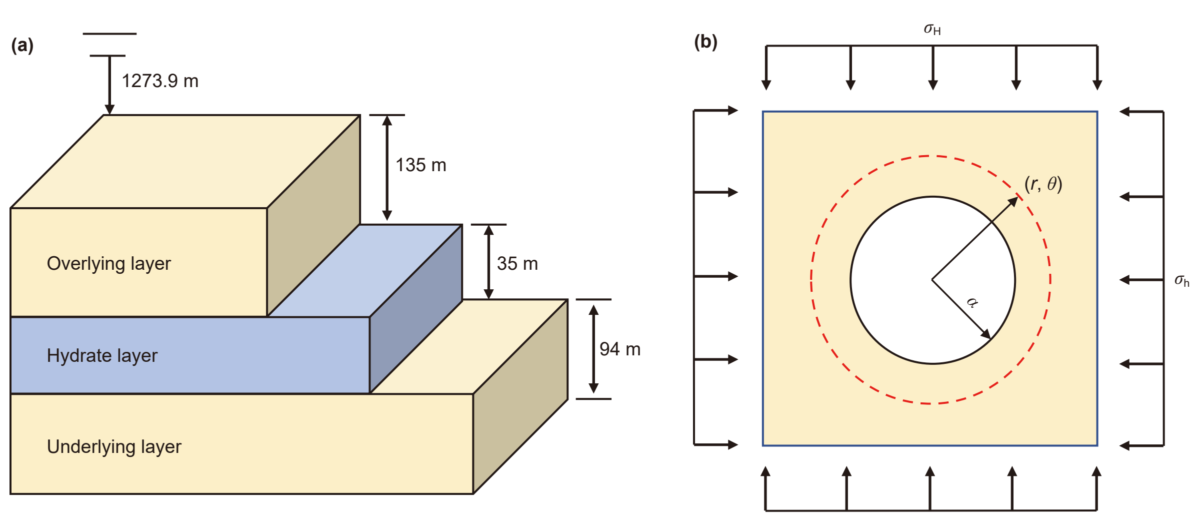

Fig. 5. Geometry of borehole trajectory in the hydrate reservoir. (**a**) Reservoir conditions and (**b**) stress distribution around the borehole.

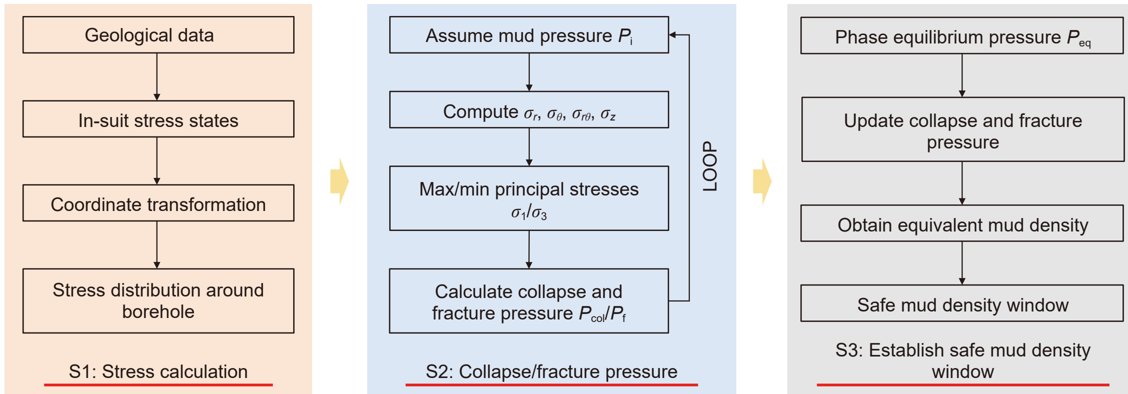

Fig. 6. Flowchart of safe drilling mud density window for hydrate reservoirs under temperature-pressure dual control.

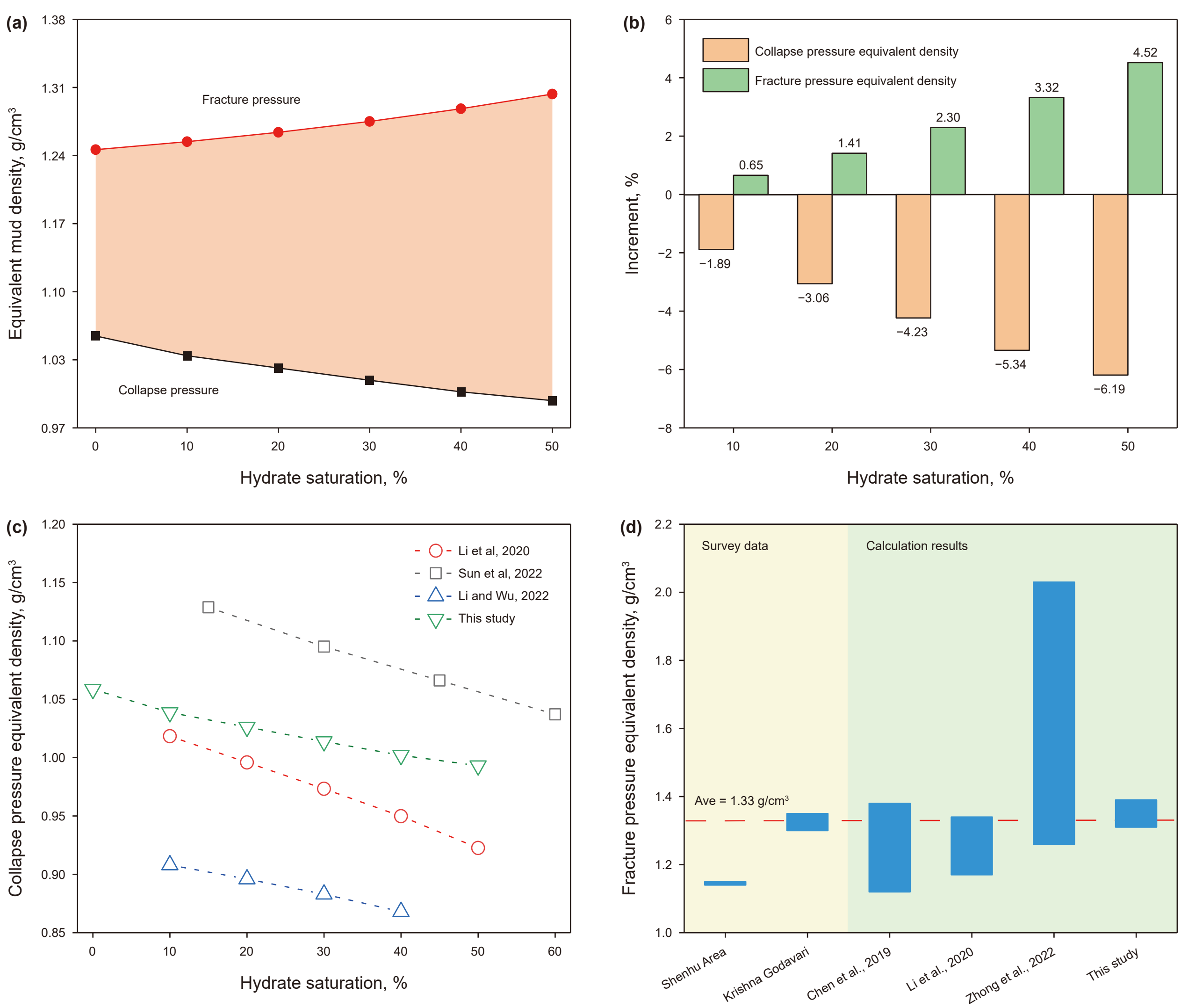

Fig. 7. Safe mud density window of hydrate reservoirs with a temperature of 288.5 K. (**a**) Equivalent mud density, (**b**) increment, (**c**) collapse pressure equivalent density, and (**d**) fracture pressure equivalent density.

controlled by coupling effects between hydrate dissociation and induced mud temperature decrease. As an endothermic reaction, hydrate dissociation can lead to a temperature drop, which may be slightly down due to high-speed circulation of drilling mud in boreholes. In general, this issue reflects the temperature sensitivity of safe mud density windows of natural gas hydrate reservoirs.

The issue becomes more complicated in the extreme conditions of equilibrium pressure exceeding fracture pressure, which requires specific discussions targeting mud temperature. The safe

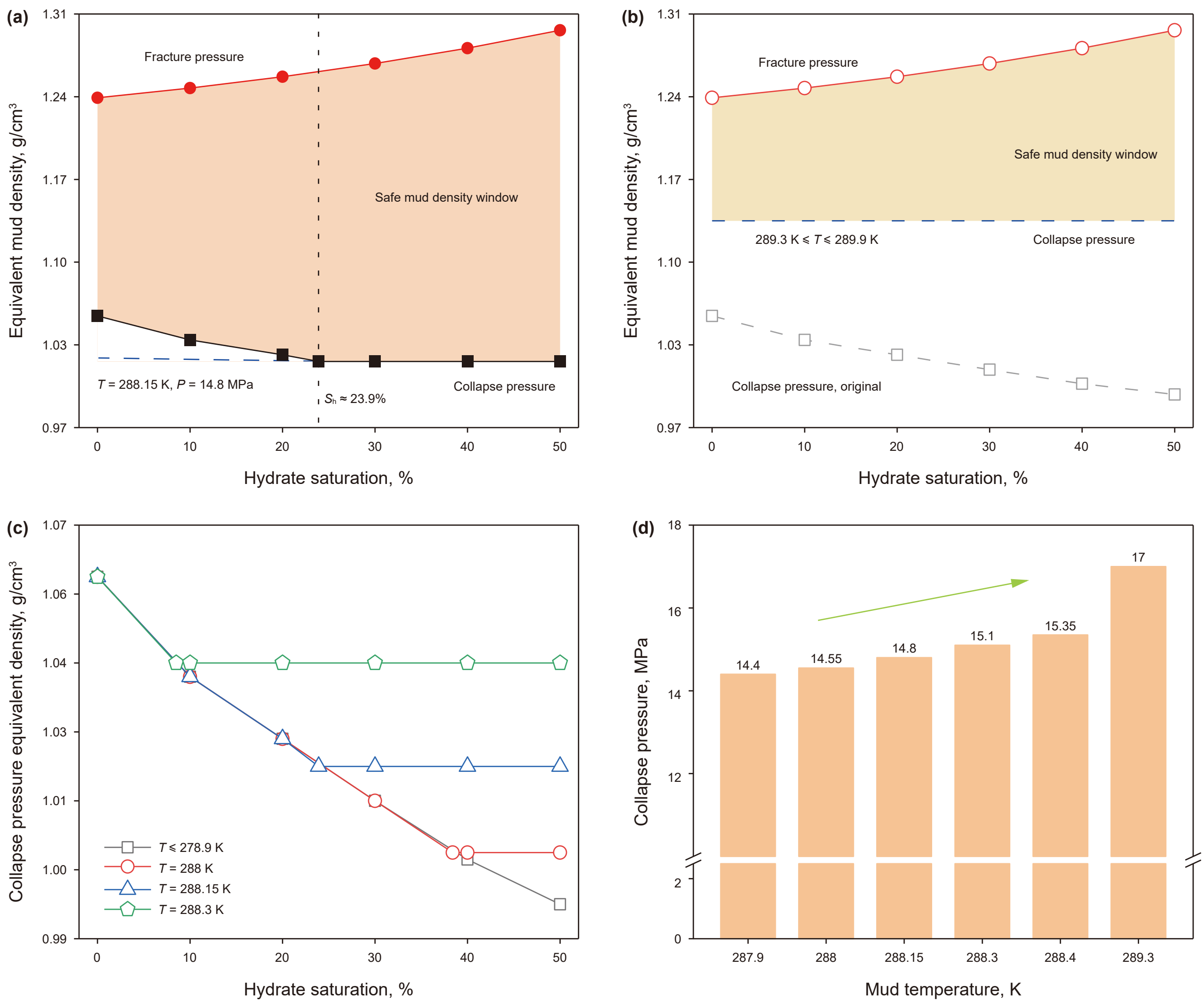

Fig. 8. Safe mud density window of hydrate reservoirs with temperature no more than 288.3 K. (**a**) Equivalent mud density (T = 288.15 K), (**b**) equivalent mud density (289.3 K $\le T \le$ 289.9 K), (**c**) variation of collapse pressure equivalent density versus mud temperature, and (**d**) variation of collapse pressure.

mud density window is divided into two sections, as displayed in Fig. 9(a). The equivalent density of collapse and fracture pressure without hydrate ($S_h = 0$) is introduced as the lower and upper limit in the left section. Wherein key point is to determine the limit of hydrate saturation S_{hl} with Eq. (20). Another right section maintains the upper limit, followed by an uncertain lower limit that can be calculated by the model. On the whole, the biggest difference between left and right sections is that the upper limit changes with varying hydrate saturation limits when the lower limit exhibits the same tendency. Especially note that try to avoid these conditions in mud density design and field operations due to enormous difficulties in downhole control.

On the contrary, there is only one section of safe mud density window once the equilibrium temperature is above the maximum fracture pressure with hydrate saturation of 0–50%. The lower and upper limits of the mud density window are defined as the collapse and fracture pressure equivalent density of hydrate-free reservoirs, as shown in Fig. 9(b). It can prevent wellbore collapse and crack formation and ensure wellbore stability.

Based on the above outcomes, insights are acquired for determining safe mud density windows during drilling hydrate reservoirs. Accurate characterization of hydrate layers is the foundation and premise for drilling design, especially hydrate saturation and heterogeneous distribution. Meanwhile, the lower limit depends on pressure and temperature of reservoirs, wherein the extreme conditions lead to various changing laws. Moreover, once uncontrolled hydrate dissociation occurs, there is no need to prevent further dissociation for both low/high hydrate-saturated layers.

4.3. *Effect of hydrate dissociation on safe mud density window*

The collapse and fracture pressure will change once the hydrate dissociates with varying temperature and pressure, the same thing with the safe mud density window. Hydrate dissociation can narrow the safe mud density window, which is decreased by ~27% on average with hydrate saturation ranging from 0 to 50%. Meanwhile, a larger dissociation degree corresponds to a narrowing magnitude of the mud density window, as illustrated in Fig. 10. That is mainly because hydrate dissociation induces strength and cohesion loss of reservoirs, causing rising collapse pressure and an opposite trend of fracture pressure.

4.4. *Effect of horizontal stress on safe mud density window*

Stress states can reflect the crustal stress field of target hydrate reservoirs that affect the wellbore instability status and proper drilling mud density, especially the intermediate principal stress.

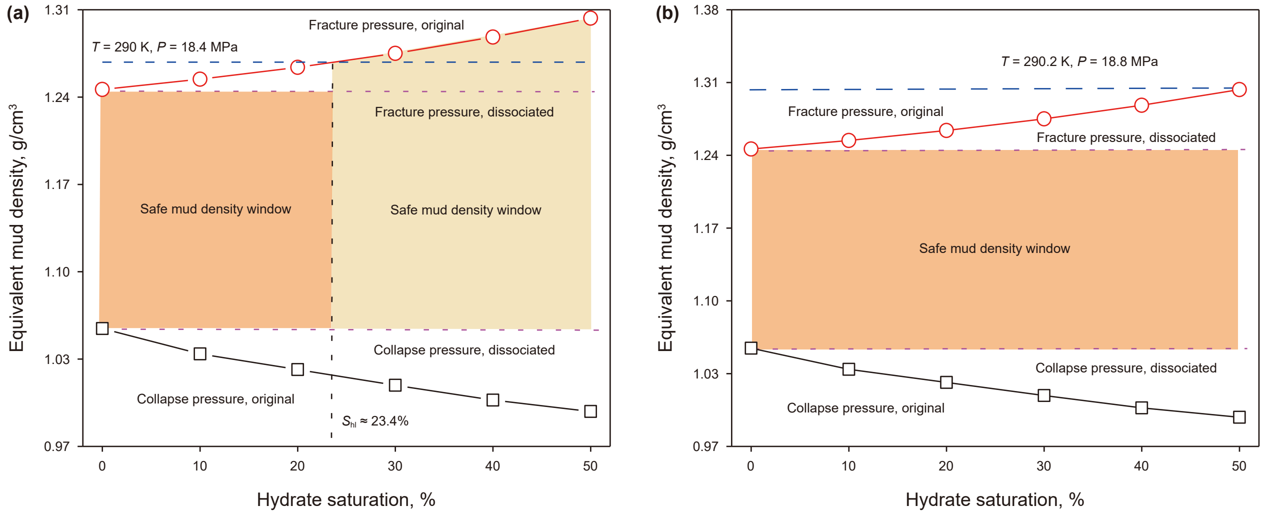

Fig. 9. Safe mud density window of hydrate reservoirs under extreme conditions. (**a**) $T = 290$ K and (**b**) $T = 290.2$ K.

Herein, we alter the intermediate principal stress with constant maximum and minimum stresses to characterize the variation of safe mud density windows.

Fig. 11 illustrates the effect of intermediate principal stress on the safe mud density window of hydrate reservoirs. Generally, higher intermediate principal stress can lead to a decrease in both

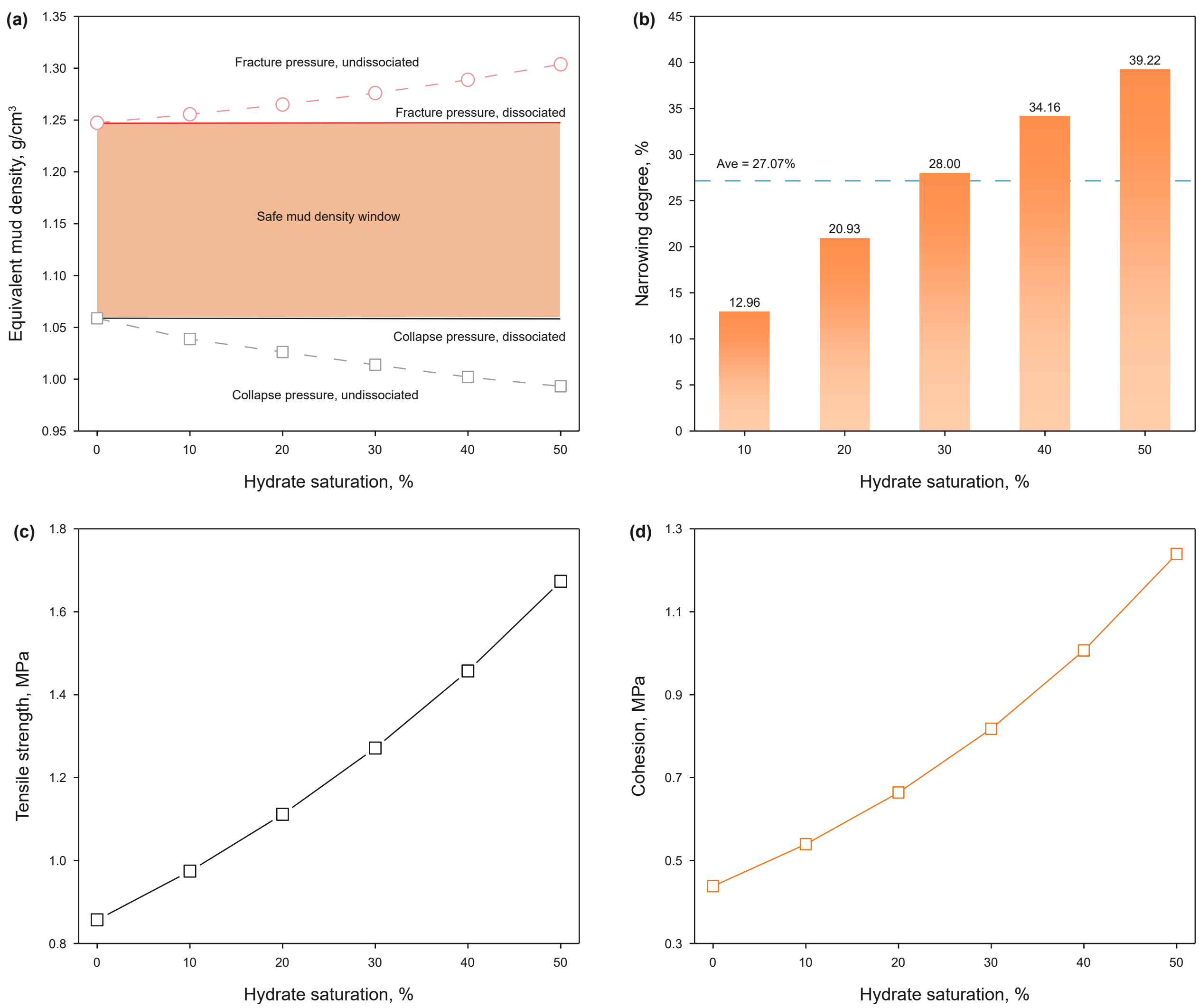

Fig. 10. Effect of hydrate dissociation on safe mud density window during drilling hydrate reservoirs. (**a**) Equivalent mud density before/after hydrate dissociation, (**b**) narrowing degree of mud density window, (**c**) tensile strength, and (**d**) cohesion of hydrate reservoirs.

equivalent density of collapse and fracture pressure, but the reduction degree differs from each other. Specifically, the decrease rate of equivalent density of fracture pressure is relatively faster than that of collapse pressure, resulting in a narrowing trend for the safe mud density window.

Additionally, hydrate dissociation may lead to more complex modes of safe mud density window affected by varying intermediate principal stress. On the one hand, it brings in a narrow window that presents a similar decreasing tendency of equivalent density of collapse and fracture pressure. On the other hand, it increases the sensitivity of equivalent density of collapse pressure to hydrate dissociation, rather than that of fracture pressure. Overall, hydrate dissociation can cause the wellbore to become unstable and trigger drilling risks.

5. Integrated control system of drilling mud density for hydrate reservoirs

Natural gas hydrate reservoirs have characteristics of shallow burial, low strength, as well as weak cementation, which correlates with drilling mud invasion, wellbore instability, blowout, leakage, and invasion damage (Li et al., 2021; Dong et al., 2024a). Different layers face different challenges due to various physical characteristics in complex reservoirs, as displayed in Fig. 12(a). Specifically, inhibiting massive dissociation is the basic task in hydrate layers (Gizatullin et al., 2023). Reducing filtration loss by forming a mud cake is required in the free gas layer, which can avoid excessive invasion of drilling mud (Merey, 2019; Sahu et al., 2020). Besides, fissure-existing intervals are in stark contrast to both hydrate and free gas layers triggered by numerous existing cracks (Albattat et al., 2022). In this regard, rapid plugging methods are conducted to inhibit the massive inflow of drilling mud by applying proper leak sealing techniques.

To deal with these problems mentioned, we propose an integrated control system based on the temperature-pressure dual control method, favoring the safe and efficient drilling process of hydrate layers, as displayed in Fig. 12(b). The dual control model is introduced into the mud system that can provide a more suitable safe mud density window design. Specifically, a new safe mud density window (yellow zone) is narrower than the previous one, which improves accuracy and reliability for mud density applied in hydrate reservoirs. Meanwhile, corresponding measures of mud-invasion prevention are presented to deal with problems occurring in free gas layers and fissure-existing intervals. As a whole, it has formed an integrated control system to avoid potential drilling risks in hydrate reservoirs.

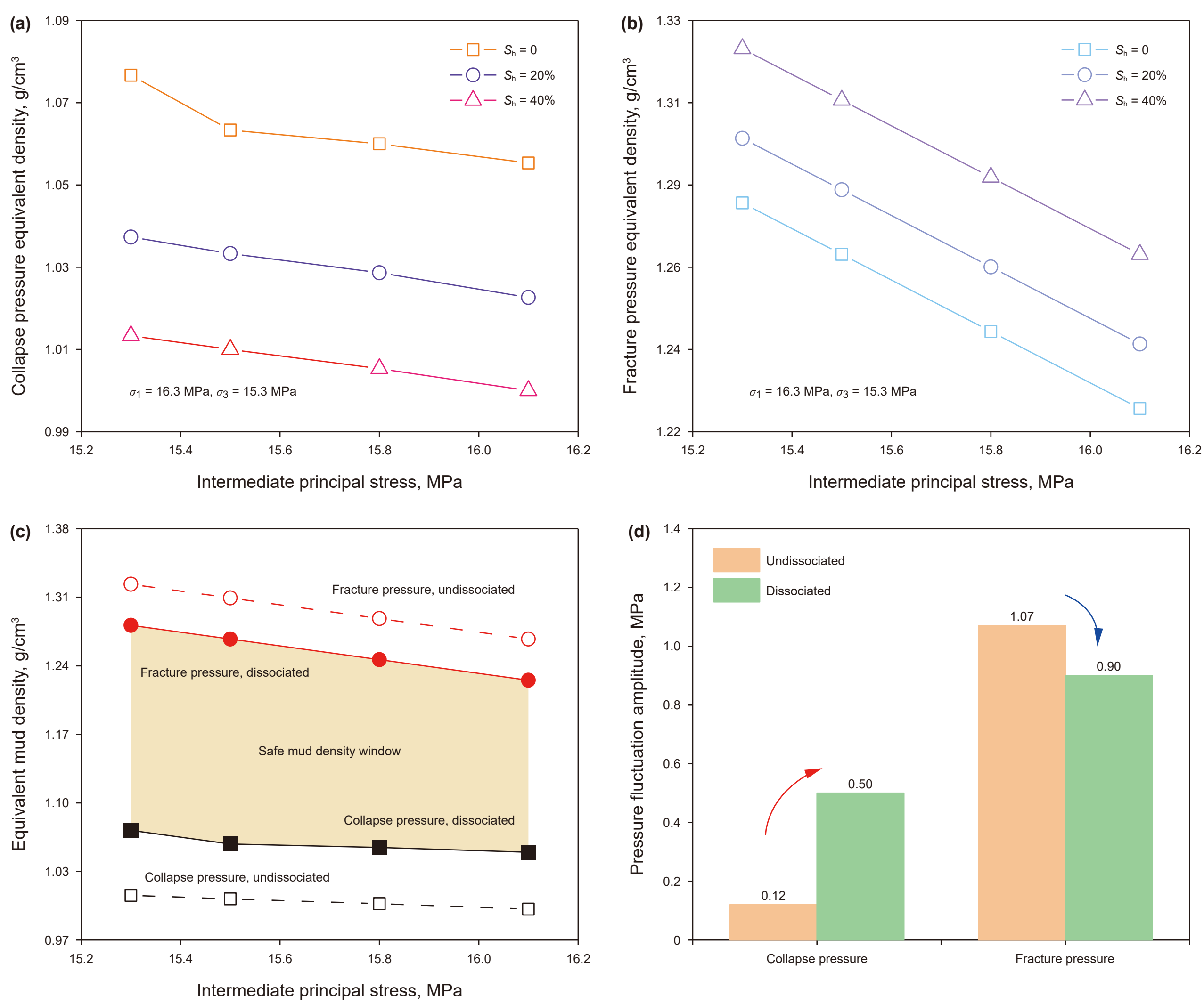

Fig. 11. Effect of hydrate dissociation on safe mud density window during drilling hydrate reservoirs. (**a**) Collapse pressure, (**b**) fracture pressure, (**c**) equivalent mud density, and (**d**) fluctuation amplitude of collapse and fracture pressure.

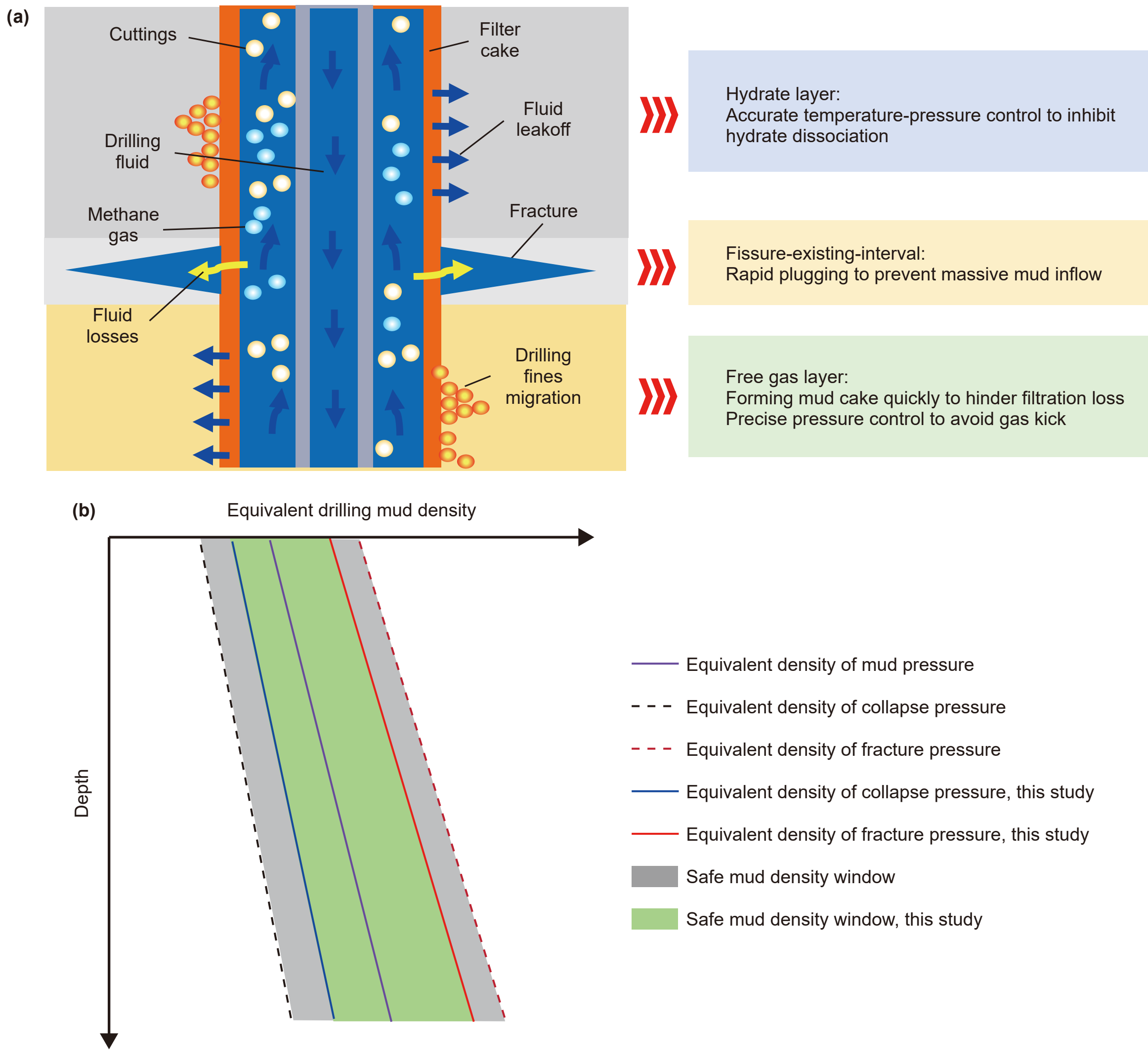

Fig. 12. An integrated mud control system with temperature-pressure dual control for drilling multi-layer hydrate reservoirs. (**a**) Challenges encountered in complex multi-layer hydrate reservoirs and (**b**) equivalent drilling mud density.

6. Conclusions

The inaccurate prediction of mud density windows can lead to drilling risks and affect the drilling process of natural gas hydrate reservoirs due to uncontrolled drilling mud invasion and massive hydrate dissociation. Herein, we propose a new model to predict safe mud weight windows by introducing the temperature-pressure dual control for drilling hydrate, which is simple, reliable, as well as accurate compared with current models. Several conclusions are summarized as follows:

Collapse pressure equivalent density decreases while fracture pressure equivalent density increases with hydrate saturation. The lower limit of the safe mud density window exhibits a relatively smaller change in amplitudes. It requires accurate characterization of heterogeneous hydrate reservoirs for proper well planning and mud density design.

Higher temperature of drilling mud can narrow safe mud weight windows. Wherein the lower limit, collapse pressure equivalent density, is more sensitive to the mud temperature than the upper limit. Extreme conditions can lead to opposite changes in the lower limit of safe mud density windows.

Hydrate dissociation narrows the safe mud density with hydrate formation. The increasing intermediate principal stress further aggravates this problem, triggered by a reduction in both lower and upper limits at different rates. Safe mud density windows are temperature sensitive due to the collapse/fracture pressure variation induced by the hydrate phase change.

An integrated mud control system involving temperature-pressure dual control is conducted to deal with filtration loss and hydrate dissociation issues during drilling multi-layer hydrate reservoirs. It can provide a better safe mud density window by introducing more accurate temperature and pressure control to avoid potential drilling risks.

CRediT authorship contribution statement

Lin Dong: Writing – original draft, Software, Investigation, Data curation, Conceptualization. **Neng-You Wu:** Writing – review & editing, Supervision, Project administration, Conceptualization. **Ke Ke:** Resources, Project administration, Funding acquisition, Formal analysis. **Li-Lin Li:** Visualization, Validation, Software, Investigation. **Yong-Chao Zhang:** Visualization, Resources, Investigation, Data curation. **Yan-Long Li:** Writing – review & editing, Supervision, Methodology, Funding acquisition.

Declaration of competing interest

The authors declare that they have no known competing financial interests or personal relationships that could have appeared to influence the work reported in this paper.

Acknowledgments

This research was supported by the NSFC Major Research Plan on West-Pacific Earth System Multispheric Interactions (No. 92358303), National Natural Science Foundation of China (Nos. U25A20798, 42506223), and project ZR2025QC376 supported by Shandong Provincial Natural Science Foundation.

References

Aadnoy, B.S., Chenevert, M.E., 1987. Stability of highly inclined boreholes. SPE Drill. Eng. 2, 364–374. https://doi.org/10.2118/16052-PA.

Abdelhafiz, M.M., Oppelt, J., Mahmoud, O., et al., 2023. Effect of drilling and wellbore geometry parameters on wellbore temperature profile: Implications for geothermal production. Adv. Geo-Energy Res. 8, 170–180. https://doi.org/10.46690/ager.2023.06.04.

Albattat, R., AlSinan, M., Kwak, H., et al., 2022. Modeling lost-circulation in natural fractures using semi-analytical solutions and type-curves. J. Petrol. Sci. Eng. 216, 110770. https://doi.org/10.1016/j.petrol.2022.110770.

Al-Shami, T.M., Jufar, S.R., Kumar, S., et al., 2023. A comprehensive review of interwell interference in shale reservoirs. Earth Sci. Rev. 237, 104327. https://doi.org/10.1016/j.earscirev.2023.104327.

Bagdeli, M., Manshad, A.K., Shadizadeh, S.R., et al., 2019. Natural fracture characterization and wellbore stability analysis of a highly fractured Southwestern Iranian oilfield. Int. J. Rock Mech. Min. Sci. 123, 104101. https://doi.org/10.1016/j.ijrmms.2019.104101.

Cheng, W., Ning, F., Sun, J., et al., 2019. A porothermoelastic wellbore stability model for riserless drilling through gas hydrate-bearing sediments in the Shenhu area of the South China Sea. J. Nat. Gas Sci. Eng. 72, 103036. https://doi.org/10.1016/j.jngse.2019.103036.

Dong, L., Li, Y., Liao, H., et al., 2020. Strength estimation for hydrate-bearing sediments based on triaxial shearing tests. J. Petrol. Sci. Eng. 184, 106478. https://doi.org/10.1016/j.petrol.2019.106478.

Dong, L., Li, Y., Wu, N., et al., 2023a. Numerical simulation of gas extraction performance from hydrate reservoirs using double-well systems. Energy 265, 126382. https://doi.org/10.1016/j.energy.2022.126382.

Dong, L., Li, Y., Zhang, Y., et al., 2024a. Deformation characteristics of hydrate-bearing sediments. J. Ocean Univ. China 23, 149–156. https://doi.org/10.1007/s11802-024-5551-y.

Dong, L., Liao, H., Li, Y., et al., 2022a. Analysis of the mechanical properties of the reconstituted hydrate-bearing clayey-silt samples from the South China Sea. J. Mar. Sci. Eng. 10, 831. https://doi.org/10.3390/jmse10060831.

Dong, L., Liu, X., Gong, B., et al., 2024b. Geomechanical properties of hydrate-bearing strata and their applications. Adv. Geo-Energy Res. 11, 161–167. https://doi.org/10.46690/ager.2024.03.01.

Dong, L., Wan, Y., Li, Y., et al., 2022b. 3D numerical simulation on drilling fluid invasion into natural gas hydrate reservoirs. Energy 241, 122932. https://doi.org/10.1016/j.energy.2021.122932.

Dong, L., Wu, N., Leonenko, Y., et al., 2023b. A coupled thermal-hydraulic-mechanical model for drilling fluid invasion into hydrate-bearing sediments. Energy 278, 127785. https://doi.org/10.1016/j.energy.2023.127785.

Dong, L., Wu, N., Leonenko, Y., et al., 2024c. Numerical analysis on hydrate production performance with multi-well systems: Synergistic effect of adjacent wells and implications on field exploitation. Energy 290, 130292. https://doi.org/10.1016/j.energy.2024.130292.

Dong, L., Wu, N., Liu, F., et al., 2024d. Estimation on strength parameters of sediments with hydrate layered distribution based on triaxial shearing tests. Gas Sci. Eng. 123, 205255. https://doi.org/10.1016/j.jgsce.2024.205255.

Fan, Y., Pang, H., Jin, Y., et al., 2025. Integration of image recognition and expert system for real-time wellbore stability analysis. Adv. Geo-Energy Res. 15, 158–171. https://doi.org/10.46690/ager.2025.02.07.

Gholami, R., Rabiei, M., Rasouli, V., et al., 2015. Application of quantitative risk assessment in wellbore stability analysis. J. Petrol. Sci. Eng. 135, 185–200. https://doi.org/10.1016/j.petrol.2015.09.013.

Gizatullin, R., Dvoynikov, M., Romanova, N., et al., 2023. Drilling in gas hydrates: Managing gas appearance risks. Energies 16, 2387. https://doi.org/10.3390/en16052387.

Gong, B., Lei, G., Chen, L., et al., 2025. Mitigating risks in deep sea gas hydrate production: A new perspective on interpreting thermo-hydro-mechanical feedbacks. Adv. Geo-Energy Res. 17, 267–270. https://doi.org/10.46690/ager.2025.09.08.

Huang, T., Li, X., Zhang, Y., et al., 2020a. Experimental study of the drilling process in hydrate-bearing sediments under different circulation rates of drilling fluid. J. Petrol. Sci. Eng. 189, 107001. https://doi.org/10.1016/j.petrol.2020.107001.

Huang, T., Zhang, Y., Li, G., et al., 2020b. Numerical modeling for drilling fluid invasion into hydrate-bearing sediments and effects of permeability. J. Nat. Gas Sci. Eng. 77, 103239. https://doi.org/10.1016/j.jngse.2020.103239.

Li, Q., 2022. Mud density optimization for horizontal well system in clayey silt hydrate reservoir with considering borehole collapse. Arabian J. Sci. Eng. 47, 11651–11671. https://doi.org/10.1007/s13369-021-06401-0.

Li, Q., Wu, J., 2022. Factors affecting the lower limit of the safe mud weight window for drilling operation in hydrate-bearing sediments in the Northern South China Sea. Geomech. Geophys. Geo-energ. Geo-resour. 8, 82. https://doi.org/10.1007/s40948-022-00396-0.

Li, Q., Liu, J., Wang, S., et al., 2024. Numerical insights into factors affecting collapse behavior of horizontal wellbore in clayey silt hydrate-bearing sediments and the accompanying control strategy. Ocean. Eng. 297, 117029. https://doi.org/10.1016/j.oceaneng.2024.117029.

Li, W., Gao, D., Yang, J., 2020. Study of mud weight window of horizontal wells drilled into offshore natural gas hydrate sediments. J. Nat. Gas Sci. Eng. 83, 103575. https://doi.org/10.1016/j.jngse.2020.103575.

Li, Y., Dong, L., Wu, N., et al., 2021. Influences of hydrate layered distribution patterns on triaxial shearing characteristics of hydrate-bearing sediments. Eng. Geol. 294, 106375. https://doi.org/10.1016/j.enggeo.2021.106375.

Lu, C., Qin, X., Sun, J., et al., 2023. Research progress and scientific challenges in the depressurization exploitation mechanism of clayey-silt natural gas hydrates in the northern South China Sea. Adv. Geo-Energy Res. 10, 14–20. https://doi.org/10.46690/ager.2023.10.03.

Merey, S., 2019. Evaluation of drilling parameters in gas hydrate exploration wells. J. Petrol. Sci. Eng. 172, 855–877. https://doi.org/10.1016/j.petrol.2018.08.079.

Moos, D., Peska, P., Finkbeiner, T., et al., 2003. Comprehensive wellbore stability analysis utilizing quantitative risk assessment. J. Petrol. Sci. Eng. 38, 97–109. https://doi.org/10.1016/S0920-4105(03)00024-X.

Motghare, P.D., Musale, A., 2017. Unconventional hydrocarbons: Gas hydrates-drilling challenges and suitable technology. In: SPE Oil and Gas India Conference and Exhibition. https://doi.org/10.2118/185424-MS.

Sahu, C., Kumar, R., Sangwai, J.S., et al., 2020. Comprehensive review on exploration and drilling techniques for natural gas hydrate reservoirs. Energy Fuel. 34, 11813–11839. https://doi.org/10.1021/acs.energyfuels.0c02202.

Sun, X., Hu, Q., Li, Y., et al., 2022. Stability characteristics of horizontal wells in the exploitation of hydrate-bearing clayey-silt sediments. J. Mar. Sci. Eng. 10, 1935. https://doi.org/10.3390/jmse10121935.

Sun, Y., Lu, H., Lu, C., et al., 2018. Hydrate dissociation induced by gas diffusion from pore water to drilling fluid in a cold wellbore. Adv. Geo-Energy Res. 2, 410–417. https://doi.org/10.26804/ager.2018.04.06.

Tian, H., Liu, W., Ding, P., et al., 2024. Numerical simulation of elastic properties of hydrate-bearing sediments with digital rock technology. Mar. Petrol. Geol. 160, 106592. https://doi.org/10.1016/j.marpetgeo.2023.106592.

Too, J.L., Cheng, A., Khoo, B.C., et al., 2018. Hydraulic fracturing in a penny-shaped crack. Part II: testing the frackability of methane hydrate-bearing sand. J. Nat. Gas Sci. Eng. 52, 619–628. https://doi.org/10.1016/j.jngse.2018.01.046.

Wan, Y., Wu, N., Hu, G., et al., 2018. Reservoir stability in the process of natural gas hydrate production by depressurization in the Shenhu area of the South China Sea. Nat. Gas. Ind. B 5, 631–643. https://doi.org/10.1016/j.ngib.2018.11.012.

Wan, Y., Yuan, Y., Zhou, C., et al., 2023. Multiphysics coupling in exploitation and utilization of geo-energy: State-of-the-art and future perspectives. Adv. Geo-Energy Res. 10, 7–13. https://doi.org/10.46690/ager.2023.10.02.

Wani, S., Samala, R., Kandasami, R.K., et al., 2023. Positioning of horizontal wellbore in the hydrate reservoir using a custom developed coupled THMC solver. Comput. Geotech. 161, 105618. https://doi.org/10.1016/j.compgeo.2023.105618.

Wei, Z., Sheng, M., Li, J., et al., 2025. Pressure diagnostics in hydraulic fracturing for unconventional completion optimization. Adv. Geo-Energy Res. 17, 196–211. https://doi.org/10.46690/ager.2025.09.03.

Yoneda, J., Kida, M., Konno, Y., et al., 2019. In situ mechanical properties of shallow gas hydrate deposits in the deep seabed. Geophys. Res. Lett. 46, 14459–14468. https://doi.org/10.1029/2019GL084668.

Zhang, J., 2013. Borehole stability analysis accounting for anisotropies in drilling to weak bedding planes. Int. J. Rock Mech. Min. Sci. 60, 160–170. https://doi.org/10.1016/j.ijrmms.2012.12.025.

Zhang, X.H., Lu, X.B., Shi, Y.H., et al., 2015. Study on the mechanical properties of hydrate-bearing silty clay. Mar. Petrol. Geol. 67, 72–80. https://doi.org/10.1016/j.marpetgeo.2015.04.019.

Zhang, Y., Liu, L., Luo, L., et al., 2025. Permeability prediction in hydrate-bearing sediments via pore network modeling. Adv. Geo-Energy Res. 16, 158–170. https://doi.org/10.46690/ager.2025.05.07.

Zhao, Y., Hu, G., Liu, L., et al., 2025. Mechanical properties of gas hydrate-bearing sediments: Research progress, challenges and perspectives. Earth Sci. Rev., 105058 https://doi.org/10.1016/j.earscirev.2025.105058.

Zheng, M., Liu, T., Jiang, G., et al., 2020. Large-scale and high-similarity experimental study of the effect of drilling fluid penetration on physical properties of gas hydrate-bearing sediments in the Gulf of Mexico. J. Petrol. Sci. Eng. 187, 106832. https://doi.org/10.1016/j.petrol.2019.106832.

Zhong, X., Nie, S., Tu, G., et al., 2024. Fracture initiation–propagation behavior of the Shenhu hydrate reservoir with connected reservoir pore water. Energy Fuel. 38, 12900–12915. https://doi.org/10.1021/acs.energyfuels.4c01973.